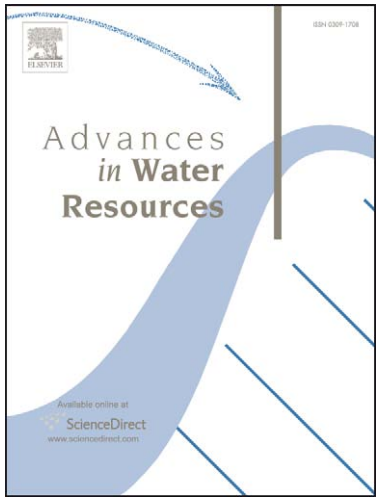

Assimilation of a ERS scatterometer derived soil moisture index in the ECMWF numerical weather prediction system

K. Scipal, M. Drusch, W. Wagner

PII: S0309-1708(08)00073-0
DOI: 10.1016/j.advwatres.2008.04.013
Reference: ADWR 1276

To appear in: *Advances in Water Resources*

Received Date: 11 December 2007
Revised Date: 30 April 2008
Accepted Date: 30 April 2008

Please cite this article as: Scipal, K., Drusch, M., Wagner, W., Assimilation of a ERS scatterometer derived soil moisture index in the ECMWF numerical weather prediction system, *Advances in Water Resources* (2008), doi: 10.1016/j.advwatres.2008.04.013

Assimilation of a ERS scatterometer derived soil moisture index in the ECMWF numerical weather prediction system

K. Scipal, M. Drusch

European Centre for Medium-Range Weather Forecasts, Reading, UK

W. Wagner

Institute of Photogrammetry and Remote Sensing, Vienna University of Technology, Vienna, Austria

Abstract

The European Centre for Medium-Range Weather Forecasts (ECMWF) currently prepares the assimilation of soil moisture data derived from advanced scatterometer (ASCAT) measurements. ASCAT is part of the MetOp satellite payload launched in November 2006 and will ensure the operational provision of soil moisture information until at least 2020. Several studies showed that soil moisture derived from scatterometer data contain skillful information. Based on data from its predecessor instruments, the ERS-1/2 scatterometers we examine the potential of future ASCAT soil moisture data for numerical weather prediction (NWP). In a first step, we compare nine years of the ERS scatterometer derived surface soil moisture index (Θ_S) against soil moisture from the ECMWF re-analysis (ERA40) data set (Θ_E) to (i) identify systematic differences and (ii) derive a transfer function which minimises these differences and transforms Θ_S into model equivalent volumetric soil moisture

Θ_S^*. We then use a nudging scheme to assimilate Θ_S^* in the soil moisture analysis of the ECMWF numerical weather prediction model. In this scheme the difference between Θ_S^* and the model first guess Θ_{FG}, calculated at 1200 UTC, is added in 1/4 fractions throughout a 24 hour window to the model resulting in analysed soil moisture Θ_{NDG}. We compare results from this experiment against those from a control experiment where soil moisture evolved freely and against those from the operational ECMWF forecast system, which uses an optimum interpolation scheme to analyse soil moisture. Validation against field observations from the Oklahoma Mesonet, shows that the assimilation of Θ_S^* increases the correlation from 0.39 to 0.66 and decreases the RMSE from 0.055 m^3m^{-3} to 0.041 m^3m^{-3} compared against the control experiment. The corresponding forecasts for low level temperature and humidity improve only marginally compared to the control experiment and deteriorate compared to the operational system. In addition, the results suggest that an advanced data assimilation system, like the Extended Kalman Filter, could use the satellite observations more effectively.

Key words: soil moisture, scatterometer, data assimilation, numerical weather prediction

PACS:

1 Introduction

In November 2006, the European Organisation for the Exploitation of Meteorological Satellites (EUMETSAT) launched MetOp-A the first out of three satellites of EUMETSAT's polar system (EPS). One of the instruments onboard the satellite is the advanced scatterometer (ASCAT) which is the succes-

* Corresponding author.
Email address: Klaus.Scipal@ecmwf.int (K. Scipal).

sor instrument of the ERS scatterometers [1,6]. Although designed to measure wind over the ocean there is increasing evidence that the ERS and MetOp scatterometer configuration also provide measurements of surface soil moisture over land.

Currently, EUMETSAT implements an operational near real time soil moisture processor at its central processing facility [17]. The processor will facilitates the retrieval of a soil moisture index Θ_S based on the method described in [41]. It was shown in several validation studies that Θ_S contains skillful information about soil moisture [42,9,7,25]. These studies focused on a qualitative comparison between Θ_S and different datasets, showing a high agreement for tropical, dry and temperate climates. A disagreement was found in deserts and polar regions. In a more quantitative study, Ceballos et al. [5] compared root zone soil moisture derived from Θ_S with in-situ data from a field site in Central Spain and estimated a root mean square error (RMSE) of 0.04 m^3m^{-3}. In a similar study using in-situ observations from agro-meteorologic networks in Russia, Ukraine and China, Scipal [31] estimated a RMSE of 0.06 m^3m^{-3}. Recently, Θ_S was also used successfully in first agro-meteorologic assimilation experiment [45] and in hydrological [24,32], meteorological [46] and climate [16] studies.

Initial soil moisture retrievals, based on ASCAT observations, indicate that the advanced sensor design and calibration will provide accurate soil moisture information at a spatial resolution of 25 km and a sampling interval of less than two days [2]. The MetOp system will hence provide an uninterrupted flow of soil moisture information until at least 2020 and therefore offers an attractive complement to dedicated soil moisture missions like the Soil Moisture and Ocean Salinity Mission (SMOS) and the Soil Moisture Active-Passive Mission

(SMAP). Especially the operational system capabilities, the near real time processing of data and the heritage of the ERS-1/2 missions will make it a valuable monitoring tool for various applications.

The availability of an observing system that can provide accurate, routine information about surface soil moisture will help to improve our understanding of the earth system's hydrological cycle [44]. In numerical weather prediction (NWP) for example, the fundamental feedback mechanism of soil moisture has been shown for the local scale [33], the regional scale [30], and the continental to global scale [15,20]. Simplifications in the representation of land-surface processes in NWP models, however, lead to systematic errors in the soil moisture field. Specifically, it was observed that free running soil moisture models tend to drift, leading to too dry boundary layer conditions [37,13]. To compensate for this effect NWP centres introduced systems to analyse soil moisture using 2 m temperature (T_{2m}) and 2 m relative humidity (RH_{2m}) as proxy observations. In the NWP context, the term analysis expresses the production of an image of the true state of the system at a given time using a combination of a dynamic model and distributed observations via a data assimilation scheme. The analysis itself can, subsequently, be used as a pseudo observation or as initial condition for a forecast. The assimilation methods for the soil moisture analysis comprise, for example, nudging schemes (e.g. UK Met Office), optimum interpolation (e.g. Meteo France), or an extended Kalman filter (e.g. German Weather Service). At ECMWF, an optimum interpolation is currently in use [23]. This scheme efficiently improves the turbulent surface fluxes and the weather forecast on large geographic domains while root zone soil moisture acts as a "sink" variable, in which errors are allowed to accumulate [12].

Direct observations of soil moisture can represent a stronger constraint in the analysis and lead to more accurate soil moisture analyses [12,29,43]. Consequently, the development of soil moisture assimilation methods has received increasing attention in recent years [43,26,27,34]. While there has been considerable progress in the development of soil moisture data assimilation methods, large-scale assimilation studies are still rare due to the paucity of suitable observations. So far, the impact of satellite retrieved soil moisture on the quality of the weather forecast has hardly been addressed. Drusch [12] used a nudging scheme to assimilate soil moisture derived from TMI satellite observations into ECMWF's Integrated Forecast System (IFS). Although the study was limited to the southern United States, he showed that the initialisation of soil moisture using satellite observations was beneficial in the soil moisture analysis. However, it was also found that the impact on the short range forecast of T_{2m} and RH_{2m} was slightly negative when compared to the operational analysis. In this study, we address the question whether we can use scatterometer derived soil moisture Θ_S to constrain the soil moisture analysis and hence to compensate for systematic errors in ECMWF's IFS on a global scale. This is of specific interest, as scatterometers have not been regarded useful for soil moisture monitoring in NWP so far. As ASCAT is not yet fully calibrated, we will base our study on data from the ERS-1/2 missions.

The study addresses two main topics (Fig. 1 shows a schematic view of the study rational and the datasets used in each step):

(1) In the first part we compare Θ_S with model volumetric soil moisture Θ_E from the ECMWF forecast system over a nine year period to identify systematic differences (section 3.1). In (section 3.2) we derive a transfer function which minimises these differences and transforms the soil

moisture index Θ_S into volumetric soil moisture Θ_S^*.

(2) In the second part (section 4) we set up three forecast experiments to study the impact of assimilating Θ_S^* in the ECMWF forecast system. These experiments are: (i) A nudging experiment (NDG), where we assimilate Θ_S^* using the methodology described in [12]; (ii) A control experiment (CTR) with an open loop configuration where soil moisture has not been analysed but evolves freely; and (iii) An experiment using the operational optimum interpolation and T_{2m} and RH_{2m} analysis increments (OI).

We evaluate the results by examining soil moisture increments (i.e. analysis-first guess) from the NDG and OI experiment (section 5.1) and by comparing the analysed soil moisture fields Θ_{NDG}, Θ_{CTR}, Θ_{OI} to field observations Θ_{OK} from the Oklahoma Mesonet (section 5.2). Finally we evaluate the impact of assimilating Θ_S^* on the forecast skill of the ECMWF NWP model (section 5.3).

2 Scatterometer derived soil moisture

The ERS scatterometers are active microwave instruments operated in C-band (5.6 GHz) at VV polarisation. ERS-1 acquired data between August 1991 and May 1996. ERS-2 was launched in March 1996 and was operated until January 2001, when due to a failure of a gyroscope all ERS-2 instruments were temporarily switched off. From 1991 until January 2001, the scatterometers achieved a daily global coverage of up to 41%. Since May 2004, ERS-2 again acquires data, however the down-link of data is limited to selected regions (i.e. North America, Europe, Northwest Africa, China and Australia). Over land

the scatterometer observations can be use to derive soil moisture information. In this study we use the soil moisture data from Vienna University of Technology's (TUWien) WARP4 archive. This data is available on a Discrete Global Grid with a resolution of 50 km and is derived by applying the TUWien model. The following paragraph gives a brief overview of the retrieval concept. For a full description of the method, the reader is referred to [39–41].

Scatterometers operating in the low frequency domain (1–10 GHz) provide a relatively direct measure of soil moisture because of their high sensitivity to the water content in the top soil layer. The challenge in retrieving soil moisture from the backscatter measurement σ^0 is to account for the effects of surface roughness and vegetation. To this end, the TUWien model exploits the unique sensor design and the advantages of a change detection method. To correct for the effects of plant growth and decay the model uses the vegetation sensitive signature of the multi-incidence angle σ^0 observations. A soil moisture index Θ_S can then be retrieved following Eq. 1, which results in a relative measure of surface (< 2 cm) soil moisture ranging between 0 and 1. In Eq. 1 σ^0_{dry} represents backscatter from the vegetated land surface under dry soil conditions, σ^0_{wet} is the corresponding measure under wet conditions.

$$\Theta_S(t) = \frac{\sigma^0(t) - \sigma^0_{dry}(t)}{\sigma^0_{wet}(t) - \sigma^0_{dry}(t)} \tag{1}$$

Assuming that σ^0_{dry} represents a completely dry and σ^0_{wet} a saturated soil surface, Θ_S is equal to the degree of saturation, which is the soil moisture content expressed in percent of porosity [18]. The reference values σ^0_{dry} and σ^0_{wet}, are estimated from the lowest and highest σ^0 values recorded during the period August 1991 to January 2001. By utilising data from a nine-year period, the reference values likely represent the respective soil conditions even in temporal

sparsely sampled areas. In extreme climates such as deserts, where saturation is not observed, a correction factor is applied to σ^0_{wet} in order to obtain spatial consistent Θ_S values. It is important to note that the method does not provide useful information if the signal is dominated by scattering from dense vegetation, water, rough topography or snow covered/frozen land surfaces. Additionally, the current implementation of the TUWien model does not explicitly incorporate azimuthal viewing effects as they are generally weak. In regions characterised by surface patterns with a distinct azimuthal orientation of the micro relief, e.g. in sand deserts, this simplification however results in an artificial modulation of the signals. To avoid the use of spurious Θ_S values we implemented a rigorous data screening. Data is rejected if the observation error of Θ_S exceeds 6%. In this context, the observation error refers to the propagation of instrument noise through the soil moisture retrieval model. The error depends on the location specific sensitivity of the microwave signal to soil moisture, to instrument noise, azimuthal viewing effects and speckle. It is the smallest expected error, assuming that the assumptions made in the retrieval method are correct. Additionally, we used the Global Lakes and Wetlands Data Base [22] to mask regions where the areal fraction of water surfaces exceeds 15% of the scatterometer footprint. Global digital elevation data from the GTOPO30 data set was used to mask regions where the normalised elevation variation within a scatterometer footprint exceeds 20%.

3 Comparison of ERS and model soil moisture

Prior to assimilation, Θ_S has to be transformed to volumetric soil moisture representing the NWP model's top soil layer. In meteorological data assimi-

lation applications this transformation is performed through the observation operator. In addition, systematic differences between the model and the observations need to be minimised to ensure an optimal analysis [8]. Although these differences at least partly stem from the model [21], corrections are often applied to the observations. In the following sections we compare Θ_S against the corresponding model fields Θ_E to identify systematic differences. For this purpose, we use data from the ECMWF re-analysis dataset (ERA40). Then we derive a transfer function which converts Θ_S into model equivalent volumetric soil moisture Θ_S^*.

The ERA40 reanalysis data set contains consistent atmosphere and surface analyses for the period from mid-1957 to 2001 based on the ECMWF NWP model [38]. Various types of observations including satellite and ground based measurements were assimilated through a 3D-Var analysis scheme. This system made use of the IFS at T159 spectral resolution ($\sim 1.125°$ horizontal spacing) with 60 vertical levels. In the IFS, land surface processes are described by the Tiled ECMWF Scheme for Surface Exchanges over Land (TESSEL) [36,19]. In TESSEL soil processes are calculated in four layers. The lower boundary of each layer is at 0.07, 0.28, 1.0 and 2.68 m depth. To keep the land surface model simple, a uniform soil type with fixed soil hydraulic parameters is used globally. Saturation is prescribed with a value of 0.472 m^3m^{-3}, field capacity with 0.323 m^3m^{-3} and the wilting point with 0.171 m^3m^{-3}.

To facilitate the comparison, Θ_S has been aggregated to the ERA40 grid and pooled into six-hourly files. The derived statistics are based on data from the period 1992–2000. Observations were masked if one of the datasets indicated missing observations or if the ERA40 reanalysis indicated a screen level temperature below 0°C and/or a snow depth larger than 0 mm. It should be noted

that the surface module of the IFS was not changed until 2007 and it can be assumed that the ERA40 climatology represents the status of the operational system at the corresponding resolution prior to 2007.

3.1 Correlations

To determine if Θ_S and Θ_E capture the same processes we calculated the correlation (R_{ABS}) between the datasets. Considering the strong seasonality of soil moisture in certain regions, R_{ABS} has to be interpreted carefully. In the Monsoon areas for example, R_{ABS} will be dominated by the strong seasonal variation, suppressing soil moisture anomalies which proceed on a much weaker magnitude. We therefore also calculate the anomaly correlation (R_{ANO}). These are obtained by removing the mean seasonal cycle in Θ_S and Θ_E derived from the nine year period. Although the nine year period is to short to calculate a robust climatology it allows us to remove the dominating effect of the seasonal cycle. The calculation of anomalies is based on a temporal identical sample population, i.e. if either Θ_S or Θ_E is missing for a specific time-step the corresponding value is removed from the other dataset. Comparing the two datasets does not provide any quantitative information about the quality of the data. However, considering that both datasets are fully independent we assume that a high correlation indicates that the same processes are captured. This assumption is valid since the simplifications in the model (e.g. a uniform soil type) and the satellite retrieval, will have a decorrelating effect.

Fig. 2 shows the spatial distribution of R_{ABS} and R_{ANO}. In general, R_{ABS} is positive over large parts of the land surface, with maximum values around 0.9.

At 85% of the land points the correlation R_{ABS} is significant at the 0.05 level, at 8% of the land points soil moisture is not correlated significantly and at 7% the correlation is negative at the 0.05 confidence level according to a t-test. For R_{ANO} these figures are similar. The spatial distribution of R_{ABS} clearly reflects zonal climate patterns. As expected, R_{ABS} is high in areas characterised by a strong seasonal soil moisture cycle (for example in the Monsoon areas). Especially over Africa R_{ANO} drops from high values around 0.9 to low values around 0.3. A possible explanation is a deficiency in the model, which can hardly be corrected through the operational analysis considering the lack of synoptic in-situ observations.

Over deserts R_{ABS} becomes negative. This problem was reported previously and can be attributed to a shortcoming of the TUWien model [42]. The maps also exhibit some unexpected features. Over Europe, R_{ABS} and R_{ANO} are comparably high. Similarly, R_{ABS} and R_{ANO} are high over South East China which is supposed to be characterised by a low sensitivity of the microwave signal to soil moisture due to a high amount of above ground biomass. In a study using soil moisture data derived from the AMSR-E radiometer, which operates in the same microwave band, the area was masked as the observations did not contain skillful information [29]. On the other hand, R_{ABS} is comparably low over the eastern parts of North America. The reason for these low correlations are not yet fully understood but can possibly be related to higher amounts of above ground biomass and hence to a higher level of noise in Θ_S. Nevertheless, there is large agreement between Θ_E and Θ_S and both datasets seem to capture the fundamental soil moisture processes.

3.2 Observation transformation

Assuming that Θ_S reflects the degree of saturation, model equivalent volumetric soil moisture can be derived by a rescaling with the model value of porosity, which is a prescribed quantity. However, such a transformation does not account for shortcomings of the model physics and the satellite retrieval method, which can result in large biases especially in the mean and variance [14,9]. Dee [8] showed that a direct assimilation of biased observations (with respect to the model) prevent a statistically optimal analysis. Therefore, we transform Θ_S with respect to the climatology of Θ_E. The transformation is accomplished by scaling Θ_S so that the cumulative distribution functions (CDF) of Θ_S and Θ_E match. In a similar study [11], the data transformation was achieved by ranking datasets of satellite derived and model soil moisture and fitting a 3^{rd} order polynomial to the differences. This approach allowed to correct differences in the mean, the variance, the skewness and the kurtosis. Here, we simplified the CDF matching to a linear transform. This effectively removes the differences in the first two moments (mean and variance). Differences in higher order moments are mainly found in dry climates. In these regions, Θ_E is more skewed towards dry values and shows a narrower distribution (i.e. a higher kurtosis). These higher order difference will enter the assimilation as an uncorrected bias. The impact of ignoring differences in higher order moments is nevertheless small and scarcely reaches values larger than 0.02 m^3m^{-3}. The disadvantage of neglecting differences in higher moments is, however, compensated by the robustness of the method especially in data sparse regions. The linear approach is also attractive as it can be fully parametrised by the mean and variance of Θ_E and Θ_S according to Eq. 2. In Eq. 2, Θ_S^* denotes

the transformed soil moisture index, Θ_S the original index from Eq. 1 and Θ_E the model soil moisture (i.e. ERA40 soil moisture). VAR denotes the variance and the bar denotes the mean of the respective sample. The intercept a and slope b are local coefficients depending on factors such as soil type, land-cover and climate. Therefore, the coefficients are derived for each model grid box independently. Spatial averaging was also omitted to minimise ergodicity errors [28].

$$\Theta_S^* = a + b \cdot \Theta_S \quad \text{with}$$
$$a = \overline{\Theta}_E - \overline{\Theta}_S \cdot \frac{VAR(\Theta_E)}{VAR(\Theta_S)}, \quad b = \frac{VAR(\Theta_E)}{VAR(\Theta_S)} \tag{2}$$

Fig. 3 shows an exemplary time series of Θ_S, Θ_S^* and Θ_E for a grid point in eastern Australia (34.3°S/148.8°E) for a one–year period. Generally, Θ_S and Θ_E capture variations induced by rainfall events observed by the nearby synoptic weather station Frogmere well. Both datasets also agree in the dry down rates. Θ_S shows a higher noise level, which is especially evident during the long dry spell in April. After applying Eq. 2 systematic differences in the dynamic range of Θ_S and Θ_E are reduced, and Θ_S^* is almost bias free with respect to Θ_E.

The transformation described in Eq. 2 uses the entire data from 1992–2000 and consequently produces bias free observations for the nine year period. This raises the question if systematic differences on seasonal to inter-annual time scales remain after the transformation. In Fig. 4 we plotted zonal means of the differences in the mean and variance of Θ_S^* and Θ_E. The differences are calculated for each month to uncover seasonal effects and for each year to reveal drifts. Although the observed differences are small on average, they exhibit organised patterns: In the tropics the monthly plots show that Θ_E is

on average slightly drier during the dry season and slightly wetter during the wet season when compared to Θ_S^*.

In the mid-latitudes, Θ_E tends to be wetter during winter and drier during summer. The most striking feature in the yearly plots is found during the winter 1996/1997 when Θ_E indicates wetter conditions than captured by Θ_S^*. Specifically, near the equatorial belt differences can reach up to 0.02 m^3m^{-3} on average. Winter 1996/1997 was an El Niño year with significantly higher temperatures and hence more precipitation in this region. This event was followed by a cold period resulting in lower precipitation rates. The observed differences suggest that the model produces stronger signals under anomalous conditions. However, the observed differences are small in terms of absolute water content. Moreover, Fig. 4 indicates that the transformation leads to consistent soil moisture estimates over time and it therefore seems reasonable to base the transformation of the satellite observations on a multi-annual data set. It is worth noting that it is possible to remove the remaining differences evident in Fig. 4 by calculating the parameters of Eq. 2 on a seasonal (yearly) basis. In this study we kept the transformation simple to retrace problems during the assimilation of Θ_S^* more directly. An optimisation of the method, considering a seasonal transformation, higher order moments and the error structure of both datasets may be inevitable in a future operational application.

4 Data Assimilation Experiments

To evaluate the impact of the satellite derived soil moisture data on the soil moisture analysis and the weather forecast we performed three data assimilation experiments. The experiments are based on ECMWF's IFS cycle 31R2

(representing the operational model version from 12 December 2006 to 05 June 2007), and make full use of the atmospheric 4D-VAR analysis system. For the sake of computational efficiency, the horizontal resolution for the three experiments is set to 125 km (spectral wave-number cutoff at 159), the vertical resolution is set to 91 layers with the lowest level at approximately ten meters. All experiments start from the same initial (operational) model state at 1 May 2005, 0000 UTC. Ten-day weather forecasts are initialised from the 0000 UTC analyses. The atmospheric variables analysed at each grid point comprise wind, temperature, humidity, and surface pressure. Roughly, five million observations from conventional sources and different satellite sensors are used in the atmospheric analysis each day. Soil moisture analyses are carried out at 0600, 1200, 1800 and 0000 UTC.

The setup of the three experiments is identical apart the way soil moisture is analysed. The first experiment (CTR), is an open loop setup where soil moisture is not constrained through an analysis and can evolve freely. In the second experiment (OI), soil moisture is analysed through the operational optimum interpolation using T_{2m} and RH_{2m} analysis increments as proxy observations [23,10,13]. Analysis increments, defined as the difference between the model first guess Θ_{FG} and the corresponding analysis, are added throughout the root zone, i.e. the top three soil layers. The first guess for the soil moisture analysis is obtained from 6 and 12-hour forecasts started at 1800 UTC and 0600 UTC. In the third experiment (NDG), the optimum interpolation scheme is replaced by a nudging scheme for the transformed soil moisture index Θ_S^* according to the method outlined in [12].

In the NDG experiment differences between daily averages of Θ_S^* and Θ_{FG} from the uppermost soil layer are computed for 1200 UTC based on a 6-hour forecast

started at 0600 UTC. The difference is then added in 1/4 fractions during the next 24-hour window at 1200, 1800, 0000 and 0600 UTC. Consequently, the full departure is added at 0600 UTC of the subsequent day. In contrast to the OI experiment, soil moisture is only added to the uppermost model layer. It should be noted that the NDG experiment assumes that the error of the soil moisture index is zero and the model error is infinite. This setting implies that the model is forced to the Θ_S^* observations and as a consequence, errors in Θ_S^* directly propagate to the model. In addition, the NDG experiment is idealised since it uses the satellite information at 1200 UTC, although the observations could also have been taken later. It is also important to notice that the assimilation concepts of the NDG and OI experiment are conceptually different. From a physical point of view the correction of soil moisture deficiencies in the OI experiment is controlled by its link to the evapotranspiration process (T_{2m} and RH_{2m} analysis increments are used as proxy observations) and it therefore explicitly adds water to the entire root zone. The assimilation scheme of the NDG experiment corrects soil moisture deficiencies directly based on surface soil moisture observations assuming that the water deficit in the root-zone is corrected in between two assimilation steps by infiltration. Although, the NDG experiment is not optimal in a statistical sense, it is a computationally inexpensive system to address the question if the scatterometer observations are useful to constrain the soil moisture analysis in a NWP model.

5 Results

Observations are used in the soil moisture analysis to correct for deficiencies in the hydrology of the model. Analysis increments, therefore, provide insight

on the spatial and temporal structure of model errors. In a first step, analysis increments from the OI experiment and the NDG experiment are compared to demonstrate the relative impact of the different observation types in the two assimilation systems and to evaluate the capability of Θ_S^* to correct for model deficiencies.

To quantify and evaluate the impact of Θ_S^* on the soil moisture analysis on the regional scale, we compare the analysed soil moisture fields from the NDG, CTR and OI experiments (Θ_{NDG}, Θ_{CTR}, Θ_{OI}) to in-situ observations Θ_{OK} from the Oklahoma Mesonet (OK Mesonet). The OK Mesonet is currently the only network providing operational soil moisture observations with a sufficient observation density over a large area (33.8°N – 37.0°N and 102.9°W – 94.6°W). It consists of over 110 automated stations measuring a variety of atmospheric and surface variables. 88 stations reported soil moisture observations on a regular basis using heat dissipation sensors. Soil moisture observations are reported every 30 minutes at depths of 0.05, 0.25, 0.60 and 0.75 m. The OK Mesonet observations are described in detail in [3].

5.1 Analysis increments

The magnitude and evolution of the analyses increments are a useful diagnostic of the forecast system. A well calibrated, physically correct model is characterised by small, randomly distributed analysis increments. Large and/or persistent increments indicate systematic model and/or observations errors. Considering that the analysis of the OI experiment effectively corrects model deficiencies [13], and that we use the same forecast model in the data assimilation experiments, we expect similar spatial and temporal patterns in

the analysis increments of the NDG experiment. However, differences in the analysis increments can be expected since:

(1) The analysis of the OI experiment adds/removes water to/from three layers, whereas the analysis of the NDG experiment only adjusts soil moisture in the surface layer. The amount of water, which can be added, is therefore confined by the thin surface layer and the nudging scheme assumes that the water is redistributed to deeper layers in between two analysis steps by infiltration.

(2) The analysis of the OI experiment corrects Θ_{FG} every six hours, whereas the analysis of the NDG experiment corrects Θ_{FG} only if the satellite overpasses the respective region, which is about once or twice per week.

In Fig. 5 we show accumulated analysis increments for May to July 2005 from the NDG and OI experiments. Considering the conceptual differences in the assimilation schemes of the NDG and OI experiment we refrain from normalising the increments based on the number of assimilation steps and/or vertical resolution as such a normalisation can not account for the non-linearity in the model-analysis system. For large parts of the world, water has been added systematically over the experiment period. In the OI experiment the water added, locally exceeds 250 mm. These values are non-negligible and represent a sizable part of the terrestrial water budget. In Spain for example, an average amount of 100 mm of water is added during the three month period which represents one quarter of the total annual amount of precipitation. Water is removed mainly over high latitudes but at lower amounts, scarcely reaching levels above 120 mm in total. The increments of the NDG experiment show similar spatial patterns as those from the OI experiment. Also the NDG experiment adds more water to the surface than the OI experiment, showing

that the root zone soil moisture can to a certain extend be controlled by infiltration. The absolute amount of water added/removed via the analysis system in the NDG experiment does, however, not reach the quantities of the OI experiment leading to a dry down of the root zone (Fig. 7). Nevertheless, the similarities in the temporal and spatial patterns of the analysis increments are evident (Fig. 5) and suggest that Θ_S^* can correct systematic errors due to an oversimplified soil parametrisation and deficiencies in the soil hydrology of the ECMWF land surface model.

5.2 Validation against OK Mesonet observations

Analysed soil moisture from the three experiments is compared against in-situ observations from the OK Mesonet. For our comparison observations are averaged to daily values. To compare analysed surface soil moisture (Θ_{NDG}, Θ_{CTR}, Θ_{OI}) of the top 0.07 m soil layer, we used OK Mesonet observations from the 0.05 m layer. For the comparison of root zone soil moisture (1 m soil layer) we calculated a weighted average of all layers where the weights corresponded to the layer depth. Error statistics (correlation, bias and standard deviation) are calculated between Θ_{OK} and Θ_{NDG}, Θ_{CTR}, Θ_{OI} time series for each station of the OK Mesonet.

The highest correlations for all stations are obtained from either Θ_{NDG} or Θ_{OI}. For 79% of the stations the highest correlation is found for Θ_{NDG}, for 21% the highest correlation is found for Θ_{OI} (Fig. 6). According to a z-test [35], the correlation of Θ_{NDG} is significantly higher in the South-East of Oklahoma in the outskirts of the Quachita mountains (significant at the 0.05 confidence level) when compared to the Θ_{CTR} and Θ_{OI} correlations. This re-

gion is characterised by forested vegetation. Stations with a higher correlation in the Θ_{OI} series are found along the major rivers of Oklahoma, the Red river in the south and the Arkansas river in the north east. However these differences are not significant at the 0.05 confidence level. The results suggest that scatterometers can contribute skill to the model even if the sensitivity of the signal towards soil moisture is attenuated by dense vegetation. On the other hand the moderate impact along the major river systems indicate that water surfaces, even if they cover only a small fraction of the satellite footprint have a non-negligible impact on the signal. The correlation coefficients are however low, and show a large spread, with an average value of 0.46±0.16 for Θ_{NDG}, 0.31±0.20 for Θ_{CTR} and 0.37±0.18 for Θ_{OI} experiment. The highest correlation of 0.57±0.15, is found for the original Θ_S^* observations. These values partly reflect the scale mismatch between coarse resolution soil moisture and in-situ point observations. Similar correlations have been reported in an assimilation study using soil moisture data form the passive microwave satellite missions AMSR-E and SMMR [29].

To account for the scaling problem we calculated regional averages for Oklahoma by spatially averaging Θ_{OK}, Θ_{CTR}, Θ_{NDG} and Θ_{OI} from all stations. The correlation coefficients for these regional time series are significantly higher with values of 0.66 for Θ_{NDG}, 0.39 for Θ_{CTR} and 0.59 for Θ_{OI}. Again, the highest correlation of 0.86, is found for Θ_S^* (area averages were only calculated if at least 2/3 of the Oklahoma area was observed by the scatterometer). These values are in line with [12], where correlation coefficients of up to 0.8 between a nudging experiment using soil moisture data form the passive microwave satellite missions TMI and OK Mesonet data were reported.

The averaged time series also show systematic differences between the exper-

iments (Fig. 7). As soil moisture in the CTR experiment is not constrained, differences are only due to the sampling mismatch and forecast model errors. The CTR experiment follows the general soil moisture trend observed during the May–July period only roughly. We observe a significant dry bias in Θ_{CTR} of 0.05 m^3m^{-3}. Beside this, the CTR experiment also fails to capture a significant soil moisture increase in the first week of July and it tends to dry down too quickly after the wet periods. The main reason for this mismatch can be found in too low rainfall rates. Rainfall in the model is persistently underestimated compared to OK Mesonet observations. In total, the model produces only 116 mm of rainfall during the May–July period, compared to an observed quantity of 222 mm. Especially the large rainfall events after 01 July 2005 are underestimated by the model. The lack of precipitation results in a persistent dry down of the root zone and consequently a large bias of 0.07 m^3m^{-3}. It should however be noted, that half of this bias is explained by differences in the initial conditions.

The analysis of the OI experiment partly compensates for these deficiencies by adding significant amounts of water to the system. This reduces the negative bias in Θ_{OI} to a value of 0.026 m^3m^{-3}. The OI analysis also partly compensates for the too quick dry downs. During the dry down in the third week of May for example this leads to more consistent soil moisture estimates. As the analysis of the OI experiment also adds water to the root zone, the dry down is impeded resulting in similar trends and the bias of 0.03 m^3m^{-3} can be fully attributed to differences in the initial conditions. Interestingly, water is also added in the period 15 June 2005 to 1 July 2005, though no precipitation was observed (Fig. 8). Comparing the total water added to the hydrologic budget through rainfall and analysis increments with the observed figures, indicates that the

analysis of the OI experiment overcompensates the shortage of soil moisture in the model. Both observations are a sign of systematic model errors.

The transformed scatterometer observations Θ_S^* follow the general trend more closely than Θ_{CTR} and Θ_{OI} do (Fig. 7). Especially during the second half of the study period, the timing of soil moisture peaks, as well as dry down rates agree well with Θ_{OK}. Differences are evident in the first week of May when the Θ_S^* is consistently drier then Θ_{OK}. This difference is possibly caused by the different vertical resolution of the scatterometer and the OK Mesonet sensors. The different vertical resolution may also explain why the scatterometer observes wet conditions around 25 May 2005 and 10 June 2005. The respective measurement coincides with rainfall events, which may have moistened the thin surface layer observed by the scatterometer, but not the deeper layers accessible to the OK Mesonet sensors. The high agreement between Θ_S^* and Θ_{OK} is expressed in a low bias of 0.01 m^3m^{-3}. Similarly, the standard deviation between Θ_S^* and Θ_{OK} is lower (0.014 m^3m^{-3}) compared to the respective values from the CTR (0.024 m^3m^{-3}) and the OI (0.019 m^3m^{-3}) experiments.

Nudging of Θ_S^* improves the analysis only slightly (Fig. 7). Although Θ_S^* forces the model toward higher soil moisture, the soil dries down rapidly after soil moisture has been added. The sampling frequency of the scatterometer seems to be insufficient to effectively constrain the model. As a result, we observe a large bias of 0.037 m^3m^{-3} of Θ_{NDG}. The standard deviation of 0.016 m^3m^{-3} is still low. It can also be observed that the amount of water added through the analysis of the NDG experiment is too little to infiltrate to the root zone, leading to too dry conditions which are similar to the CTR experiment. It is worth noting that the problem regarding the observation frequency is somewhat in contradiction to Calvet and Noilhan [4], who found that a three day

sampling interval is sufficient to constrain model soil moisture. However, in [4], soil moisture for the entire soil profile was updated using surface observations in a quasi-Newton optimisation algorithm.

5.3 Forecast Impact via Surface Fluxes

Soil moisture has a significant impact on the state of the atmosphere due to its influence on the partitioning between latent and sensible heat fluxes and consequently the screen level parameters, i.e. T_{2m} and RH_{2m}. We therefore examine the impact of the soil moisture analyses from the NDG, CTR and OI experiments on the lower atmosphere for selected areas of the globe and for the OK Mesonet. Fig. 9 shows time series of daily averaged T_{2m} and RH_{2m} for the OK Mesonet and the NDG, CTR and OI experiments. In general, the difference between observed and analysed T_{2m} and RH_{2m} is small. With respect to T_{2m} all three experiments show a high agreement to OK Mesonet observations with a correlation above 0.9 and a moderate bias of -0.5°C. Differences between the NDG, CTR and OI are marginal. For RH_{2m} differences are more pronounced, although still small. Similar to T_{2m} the correlations for RH_{2m} are high with values of 0.89, 0.85 and 0.91 for the NDG, CTR and OI experiment. However, the observed bias is substantial. The OI experiment shows the smallest bias of -6.4%. The bias for the NDG and CTR experiments are slightly larger reaching values of -7.8% and -9.3% respectively.

The effect of the soil moisture analysis on the forecast skill of screen level parameters can be assessed through objective measures such as forecast bias and correlation. Both quantities compare the forecast for a given time step against the corresponding verifying analysis. Fig. 10 shows spatial average

bias and correlation scores for the 1–5 day forecast for Europe (37°N – 55°N, 10°W – 30°E), North America (25°N – 55°N, 120°W – 75°W) and North West Africa (5°N – 18°N, 20°W – 10°E). These statistics indicate that in all three experiments the T_{2m} forecasts are better than the ones for RH_{2m}. The correlation scores for T_{2m} are well above 0.6 with significantly higher values for Europe and North America. For RH_{2m} the forecast correlations exceed 0.6 only for the first two days and then drop to lower values. For both parameters, differences in the correlation for the CTR, NDG and OI experiments are small. Again, the biases show substantial differences: over Europe and North America a warm T_{2m} bias can be observed in the model forecast. Over North West Africa the bias becomes negative indicating that the model predicts cooler conditions. For all three regions, the OI experiment predicts lower T_{2m} than the NDG and CTR experiments. The observed difference is 0.25°C on average and reaches high values of 0.5°C over North America. The RH_{2m} bias is negative for Europe and North America, i.e. the model predicts less humid conditions. For both regions, the values are similar, and the CTR experiment shows higher correlations. Over North West Africa, more humid conditions are predicted by the model after day two of the forecast. Interestingly, over North West Africa the OI experiment is outperformed by the NDG and CTR experiments. This might be related to the fact that the NDG and CTR experiment generally predict warmer, less humid conditions, which are closer to real conditions in this region during the study period.

6 Conclusions & Perspectives

ECMWF's current soil moisture analysis system is based on an optimum interpolation scheme of 2 m temperature (T_{2m}) and 2 m relative humidity (RH_{2m}). It was shown by Drusch [13] that this scheme efficiently improves the turbulent surface fluxes and the weather forecast on large geographic domains while root zone soil moisture acts as a "sink" variable, in which errors are allowed to accumulate. Satellite observations provide more direct estimates of surface soil moisture conditions which can complement the classical soil moisture analysis. In this study we addressed the question if an ERS scatterometer derived soil moisture index Θ_S can improve the soil moisture analysis in the ECMWF Integrated Forecast System. For this purpose, we compared soil moisture analyses based on the nudging of Θ_S (NDG experiment) with soil moisture analyses based on the optimum interpolation of T_{2m} and RH_{2m} (OI experiment) and soil moisture analysis of an open loop configuration where the surface analysis is not constrained by observations (CTR experiment). The results of this study suggest:

(1) Scatterometer observations contain valuable information about surface soil moisture. A comparison with nine years of model soil moisture from the ERA40 re-analysis indicates a correlation of up to 0.9 for absolute and 0.7 for anomalies over large parts of the land surface. Comparison with in-situ observations from the OK Mesonet confirms the high accuracy of Θ_S and suggests that Θ_S can be regionally more accurate than ECMWF's NWP model.

(2) A scheme to transform Θ_S to model equivalent volumetric surface soil moisture Θ_S^* based on Cumulative Distribution Function matching has

been presented. It has been shown that the high agreement of the climatological characteristics of Θ_S and the ERA40 soil moisture Θ_E justifies the application of a linear transform.

(3) Based on a comparison with in-situ observations of the OK Mesonet we showed that the assimilation of Θ_S^* has a positive impact on the soil moisture analysis. However, the nudging scheme can not compensate for the high evaporation rate of the model leading to too low soil moisture conditions in the root zone. Problems are related to the revisit time of the ERS scatterometer, which is once to twice per week over the OK Mesonet region, and the fact that the analysis of the NDG experiment only adds water to the surface layer of the model. This problem is not observed in the operational OI configuration which uses T_{2m} and RH_{2m} analysis increments to update the entire root zone.

(4) The lack of water added during the analysis to the root zone is detrimental to the prediction of T_{2m} and RH_{2m}. In general, the impact of Θ_S^* on the prediction of T_{2m} and RH_{2m} is slightly positive when compared to the CTR experiment. When compared to the operational model (OI experiment), we observe drier, less humid conditions, and the forecast skill for screen level parameters is reduced.

In a study by Drusch [12] the problem of the dry down of the root zone was not observed in a similar extend. The study used the same experimental setup and soil moisture data derived from the passive microwave satellite mission TMI. TMI revisist the Oklahoma region daily. This leads to a stronger constraint of the root zone soil moisture of the model and consequently also leads to improved forecasts of screen level parameters when compared to results of this study. Apart from this difference the results are comparable. It is therefore

expected that the analysis system will benefit from the higher observation frequency of the MetOp scatterometer.

In addition, improvements are expected from the use of the Extended Kalman Filter technique. The Extended Kalman Filter considers the observation and model errors during the analysis in a statistically optimal way and allows to assimilate the observation at the correct observation time. The Extended Kalman Filter also allows to combine the assimilation of T_{2m}, RH_{2m} and satellite observations as proposed by [34] and hence takes full advantage of all available data. However, combining the different data sets in the Extended Kalman Filter is a major challenge considering that the temporal and spatial structure of model and observation errors need to be known precisely.

Acknowledgements

This project has partly been funded through EUMETSAT's Hydrology Satellite Application Facility H-SAF. ERS scatterometer data was processed within the Austrian Science Fund project L148-N10 GLOBESCAT. The field observation database was kindly provided by the Oklahoma Mesonet System. At ECMWF Erik Andersson, Gianpaolo Balsamo and Patricia DeRosany provided helpful comments on the manuscript and Rob Hine helped with the final preparation of the figures.

References

[1] Anderson, C., J. Figa-Saldaña, J. J. W. Wilson, R. Gelsthorpe, and E. Attema. The advanced scatterometer (ASCAT) on the MetOp satellites: An operational

follow-on to ESA ERS C-band scatterometers, in Envisat ERS Symposium, ESA Special Publication, 2005, vol. 572.

[2] Bartalis, Z., W. Wagner, V. Naeimi, S. Hasenauer, K. Scipal, H. Bonekamp, J. Figa, and C. Anderson. Initial soil moisture retrievals from the MetOp-A advanced scatterometer (ASCAT), Geophys. Res. Let., 2007, 34, L20401, doi:10.1029/2007GL031088.

[3] Basara, J., and T. Crawford. Improved installation procedure for deep-layer soil moisture measurements, J. Atmos. Ocea. Tech., 17, 879–884.

[4] Calvet, J. C., and J. Noilhan. From near-surface soil moisture to root zone soil moisture using year-round data, J. Hydromet., 1, 393–411.

[5] Ceballos, A., K. Scipal, W. Wagner, J. Martinez-Fernandez. Validation of ERS scatterometer-derived soil moisture data over the central part of the Duero Basin, Spain, Hydrol. Proc., 2005, 19(8), 1549–1566.

[6] Cohen, H. The EUMETSAT Polar System - a major step for operational meteorology, ESA Bulletin, 2006, 127, 18–23.

[7] Crow, W. T., and X. Zhan. Continental-scale evaluation of remotely sensed soil moisture products, IEEE Geosc. Rem. Sens. Let., 2007, 4, 451–455.

[8] Dee, D., and A. daSilva. Data assimilation in the presence of forecast bias, Q. J. Roy. Met. Soc., 1998, 124, 269–295.

[9] Dirmeyer, P. A., Z. Guo, and X. Gao. Comparison, validation, and transferability of eight multiyear global soil wetness products, J. Hydromet., 2004, 5, 1011–1033.

[10] Douville, H., P. Viterbo, J.-F. Mahfouf, and A. Beljaars. Evaluation of the optimum interpolation and nudging technique for soil moisture analysis using FIFE data, Mon. Wea. Rev., 2000, 128, 1733–1756.

[11] Drusch, M., E. F. Wood, and H. Gao. Observation operators for the direct assimilation of TRMM microwave imager retrived soil moisture, Geophys. Res. Let., 2005, 32, L15403, doi:10.1029/2005GL023623.

[12] Drusch, M. Initializing numerical weather prediction models with satellite-derived surface soil moisture: Data assimilation experiments with ECMWF's Integrated Forecast System and the TMI soil moisture data set, J. Geophys. Res., 2007, 112, D03102, doi:10.1029/2006JD007478.

[13] Drusch, M. and P. Viterbo. Assimilation of screen-level variables in ECMWF's Integrated Forecast System: A study on the impact on the forecast quality and analysed soil moisture, Mon. Wea. Rev., 2007, 135, 300–314.

[14] Entin, J., A. Robock, K. Y. Vinnikov, S. Qiu, V. Zabelin, S. Liu, A. Namkhai and T. Adyasuren. Evaluation of global soil wetness project soil moisture simulations, J. Met. Soc. Japan, 1999, 77, 183–198.

[15] Ferranti, L., and P. Viterbo. The European summer of 2003: Sensitivity to soil water initial conditions, J. Climate, 2006, 19, 3659–3680.

[16] Fontaine, B., S. Louvet, and P. Roucou. Fluctuations in annual cycles and inter-seasonal memory in west africa: Rainfall, soil moisture and heat fluxes, Theo. Appl. Clim., 2006, 88, 57–70.

[17] Hasenauer, S., W. Wagner, K. Scipal, V. Naeimi, and Z. Bartalis. Implementation of near-real-time soil moisture products in the SAF network based on MetOp ASCAT data, in EUMETSAT Meteorological Satellite Conference, 2006.

[18] Hillel, D. Introduction to Soil Physics, Academic Press, 1980.

[19] van den Hurk, B., P. Viterbo, A. Beljaars, and A. Betts. Offline validation of the ERA40 surface scheme, ECMWF Technical Memorandum, European Centre for Medium Range Weather Forecasts, 2000.

[20] Koster, R., and the GLACE Team. Regions of strong coupling between soil moisture and precipitation, Science, 2004, 305, 1138–1140, doi:10.1126/science.1100217.

[21] Koster, R., and P. C. D. Milly. The interplay between transpiration and runoff formulation in land surface schemes used with atmospheric models, J. Climate, 2007, 10, 1578–1591.

[22] Lehner, B., and P. Döll. Development and validation of a global database of lakes, reservoirs and wetlands. J. Hydro., 2004, 296, 1–22.

[23] Mahfouf, J.-F., Analysis of soil moisture from near surface paarmeters: A feasability study, J. Appl. Met., 1991, 30, 1534–1547.

[24] Parajka, J., V. Naeimi, G. Blöschl, W. Wagner, R. Merz, and K. Scipal. Assimilating scatterometer soil moisture data into conceptual hydrologic models at the regional scale, Hydr. Earth Sys. Sci., 2006, 10(3), 353–368.

[25] Pellarin, T., J. C. Calvet, and W. Wagner. Evaluation of ERS scatterometer soil moisture products over a half degree region in southwestern France, Geophys. Res. Let., 2006, 33, L17401, doi:10.1029/2006GL027231.

[26] Reichle, R., D. McLaughlin, and D. Entekhabi. Hydrologic data assimilation with the ensemble Kalman filter, Mon. Wea. Rev., 2002a, 130, 103–114.

[27] Reichle, R., J. Walker, R. Koster, and P. Houser. Extended versus ensemble Kalman filtering for land data assimilation, J. Hydromet., 2002b, 3, 728–740.

[28] Reichle, R. H., and R. D. Koster. Bias reduction in short records of satellite soil moisture, Geophys. Res. Let., 2004, 31, L19501, doi:10.1029/2004GL020938.

[29] Reichle, R. H., R. D. Koster, P. Liu, S. P. P. Mahanama, E. G. Njoku, and M. Owe. Comparison and assimilation of global soil moisture retrievals from the advanced microwave scanning radiometer for the earth observing system

(AMSR-E) and the scanning multichannel microwave radiometer (SMMR), J. Geophys. Res., 2007, 112, D09108, doi:10.1029/2006JD008033.

[30] Schär, C., D. Lüthi, U. Beyerle, and E. Hise. The soil precipitation feedback: A process study with a regional climate model, J. Climate, 1999, 12, 722–741.

[31] Scipal, K. Global Soil Moisture Retrieval from ERS Scatterometer Data, PhD thesis, Vienna University of Technology, 2002

[32] Scipal, K., C. Scheffler, and W. Wagner. Soil moisture-runoff relation at the catchment scale as observed with coarse resolution microwave remote sensing, Hydr. Earth Sys. Sci., 2005, 9(3), 173–183.

[33] Seuffert, G., P. Gross, C. Simmer, and E. Wood. The influence of hydrologic modelling on the predicted local weather: Two-way coupling of a mesoscale weather prediction model and a land surface hydrologic model, J. Hydromet., 2002, 3, 505–523.

[34] Seuffert, G., H. Wilker, P. Viterbo, M. Drusch, and J.-F. Mahfouf. The usage of screen-level parameters and microwave brightness temperature for soil moisture analysis, J. Hydromet., 2004, 5, 516–531.

[35] Sprinthall, R. C. Basic Statistical Analysis: Seventh Edition, 2003, Pearson Education Group.

[36] Viterbo, P., and A. Beljaars. An improved land surface parameterization scheme in the ECMWF model and its validation, J. Climate, 11, 2716-2748, 1995.

[37] Viterbo, P. The representation of surface processes in general circulation models, Ph.D. thesis, University of Lisbon, 1996.

[38] Uppala, S.M., and 45 co-authors. The ERA-40 re-analysis. Q. J. Roy. Met. Soc., 2005, 131, 2961–3012.

[39] Wagner, W., G. Lemoine, M. Borgeaud, and H. Rott. A study of vegetation cover effects on ERS scatterometer data, IEEE Trans. Geosc. Rem. Sens., 1999, 37, 938–948.

[40] Wagner, W., J. Noll, M. Borgeaud, and H. Rott. Monitoring soil moisture over the Canadian Prairies with the ERS scatterometer, IEEE Trans. Geosc. Rem. Sens., 1999, 37, 206–216.

[41] Wagner, W., G. Lemoine, and H. Rott. A method for estimating soil moisture from ERS scatterometer and soil data, Rem. Sens. Env., 1999, 70, 191–207.

[42] Wagner, W., K. Scipal, C. Pathe, D. Gerten, W. Lucht, and B. Rudolf. Evaluation of the agreement between the first global remotely sensed soil moisture data with model and precipitation data. J. Geophys. Res. (Atm.), 2003, 108(D19), 4611, doi:10.1029/2003JD003663.

[43] Walker, J., and P. Houser. A methodology for initializing soil moisture in a global climate model: Assimilation of near-surface soil moisture observations, J. Geophys. Res., 2001, 106(D11), 11761–11774.

[44] Wei, M.-Y.. Soil moisture: Report of a workshop held in Tiburon, California, 25-27 January 1994, in NASA Soil Moisture Workshop, NASA Conference Publication, 1994, vol. 3319.

[45] de Wit, A. J. W., and C. A. van Diepen. Crop model data assimilation with the ensemble Kalman filter for improving regional crop yield forecasts, Agr. Forest Met., 2007, 146, 38–56.

[46] Zhao, D., B. Su, M. Zhao. Soil moisture retrieval from satellite images and its application to heavy rainfall simulation in eastern China, Adv. Atmos. Sc., 2006, 23, 299–316.

Fig. 1. Schematic view of the experimental setup.

Fig. 2. Correlation between the scatterometer derived soil moisture index Θ_S and ERA40 reanalysis soil moisture Θ_E for (a) absolute values and (b) anomalies for the period 1991 to 2001.

Fig. 3. (a) The scatterometer derived soil moisture index Θ_S (diamonds, right x-axis scale), transformed soil moisture index Θ_S^* (black line) and model soil moisture Θ_E from the ERA40 reanalysis (grey line) in eastern Australia (34.3°S/148.8°E). (b) Observed rainfall and temperature range at the nearby synoptic weather station Frogmere.

Fig. 4. Hovmöller diagram of differences in the mean and variance between model soil moisture Θ_E from the ERA40 reanalysis and the transformed scatterometer derived soil moisture Θ_S^*. The diagrams show (a) monthly differences of the mean; (b) monthly differences of the variance; (c) yearly differences of the mean; (d) yearly differences of the variance.

Fig. 5. (a) Accumulated surface soil moisture increments for the OI experiment for the period May, June, July 2005. Red colour tones indicate that water is removed, blue colour tones indicate that water is added during the analyses. (b) Same as (a), but for the entire root zone; (c) Same as (a), but for the NDG experiment. (d) Number of assimilation steps in the NDG experiment.

Fig. 6. Performance of time series correlation for each station of the Oklahoma Mesonet. Triangle symbols indicates that the correlation is highest for Θ_{NDG}. Circle symbols indicates that the correlation is highest for Θ_{OI}. Filled symbols indicate that the correlation is significantly higher at the 0.05 confidence level than the correlation from the other two experiments.

Fig. 7. (a) Station average rainfall observed at the OK Mesonet (black) and from the CTR experiment (grey). (b) Station average surface soil moisture Θ_{OK} (solid black), Θ_{NDG} (solid grey), Θ_{CTR} (thick dashed) and Θ_{OI} (thin dashed). Diamonds display Θ_S^* observations. (c) Same as (b) but for the root zone.

Fig. 8. Time series of accumulated rainfall and soil moisture increments from the NDG experiment (light grey) and the OI experiment (dark grey). Solid lines show accumulated rainfall, dashed lines accumulated soil moisture increments. Dotted lines show the total amount of water added to the system through rainfall and soil moisture increments. The black line shows the accumulated precipitation observed at the OK Mesonet.

Fig. 9. (a) Time series of RH_{2m} and (b)T_{2m} for the NDG (solid grey), CTR (thick dashed) and OI (thin dashed) experiment and OK Mesonet observations (black). The time series show daily averaged data based on 0000, 0600, 1200 and 1800 UTC analyses.

Fig. 10. (a) Correlation scores of T_{2m} forecasts; (b) Bias scores of T_{2m} forecasts; (c) Correlation scores of RH_{2m} forecasts; (d) Bias scores of RH_{2m} forecasts. Scores are averaged for Europe (solid line) North America (dashed line) and North West Africa (dotted line). Different grey tones show scores for the NDG (light grey), CTR (black) and OI (dark grey) experiment.

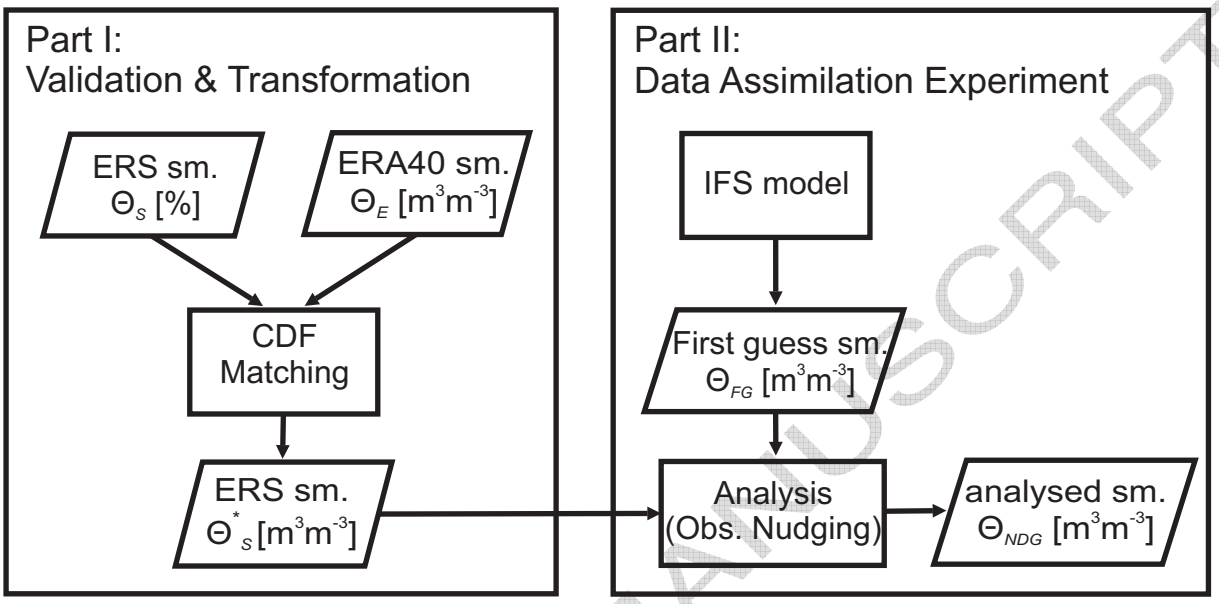

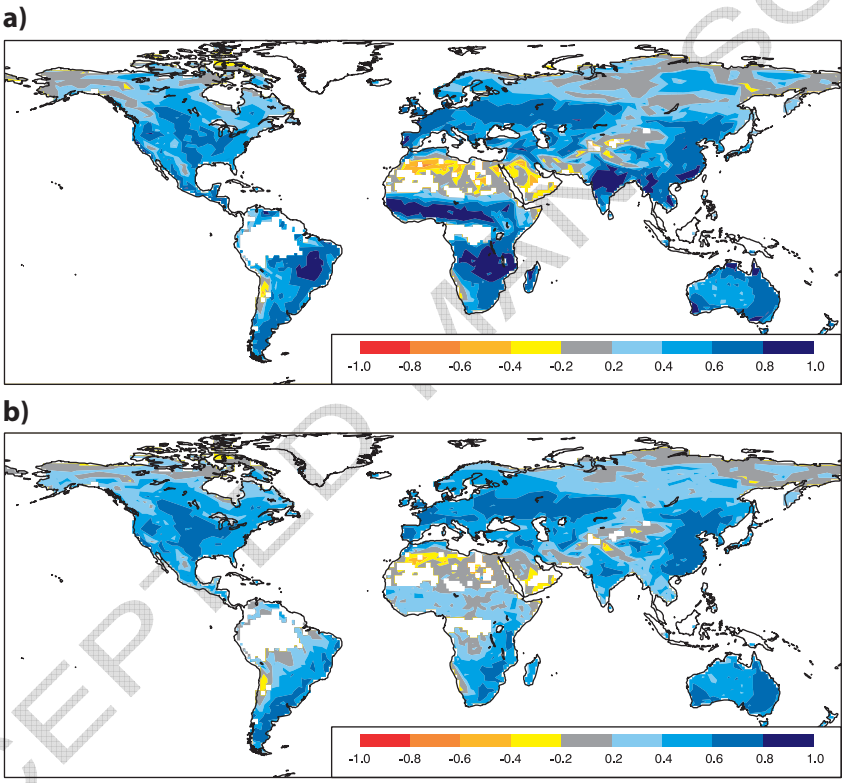

Fig. 2.

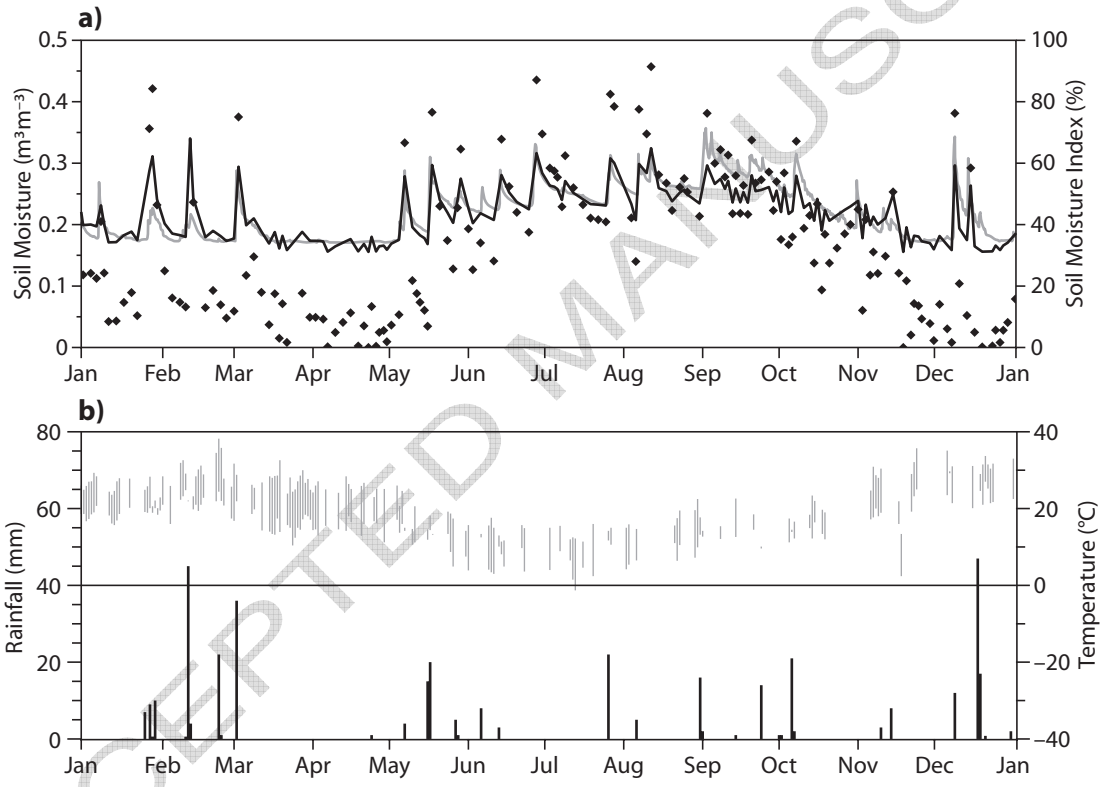

Fig. 3.

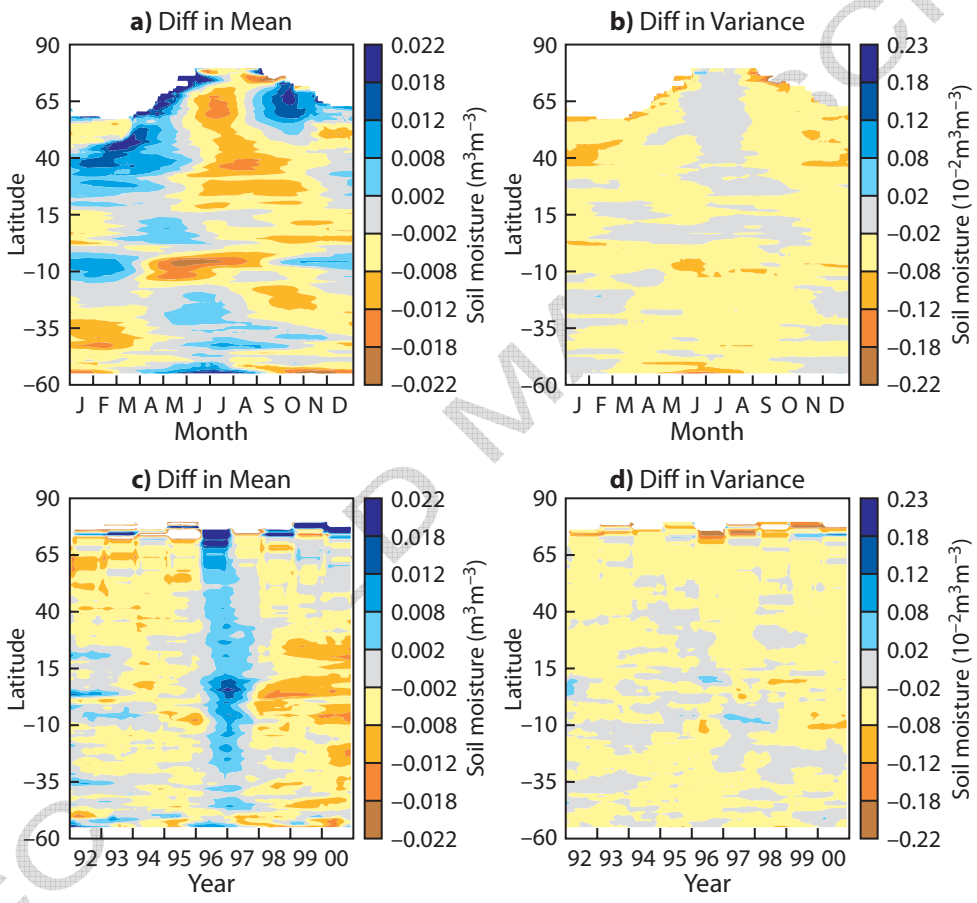

Fig. 4.

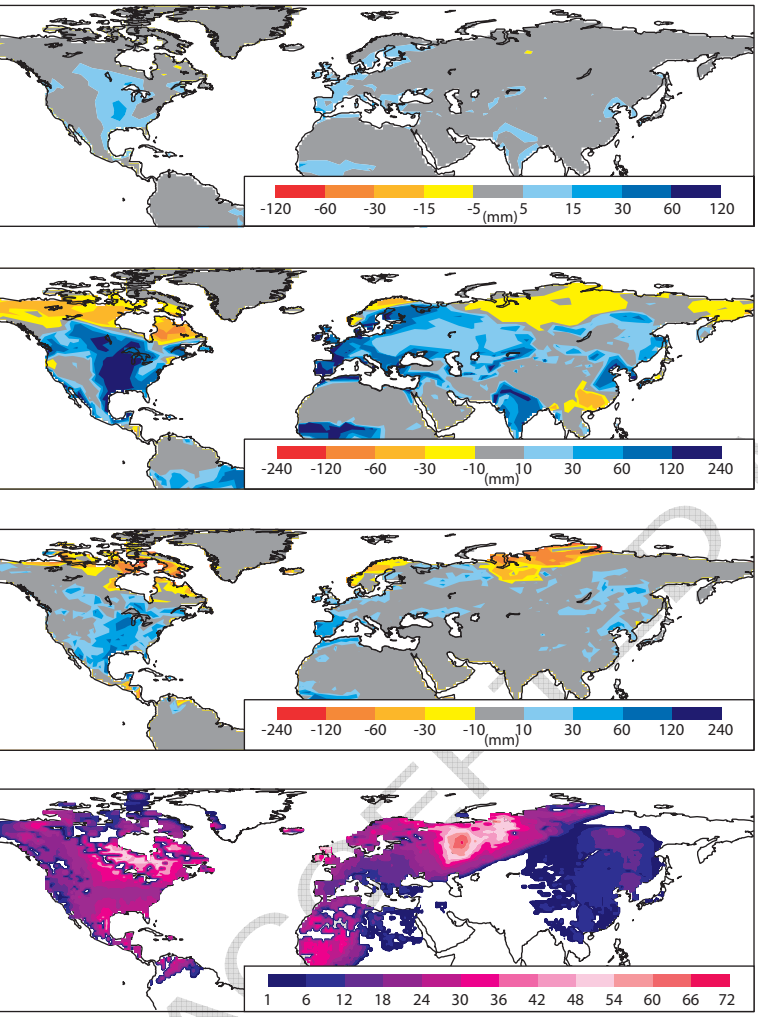

Fig. 5.

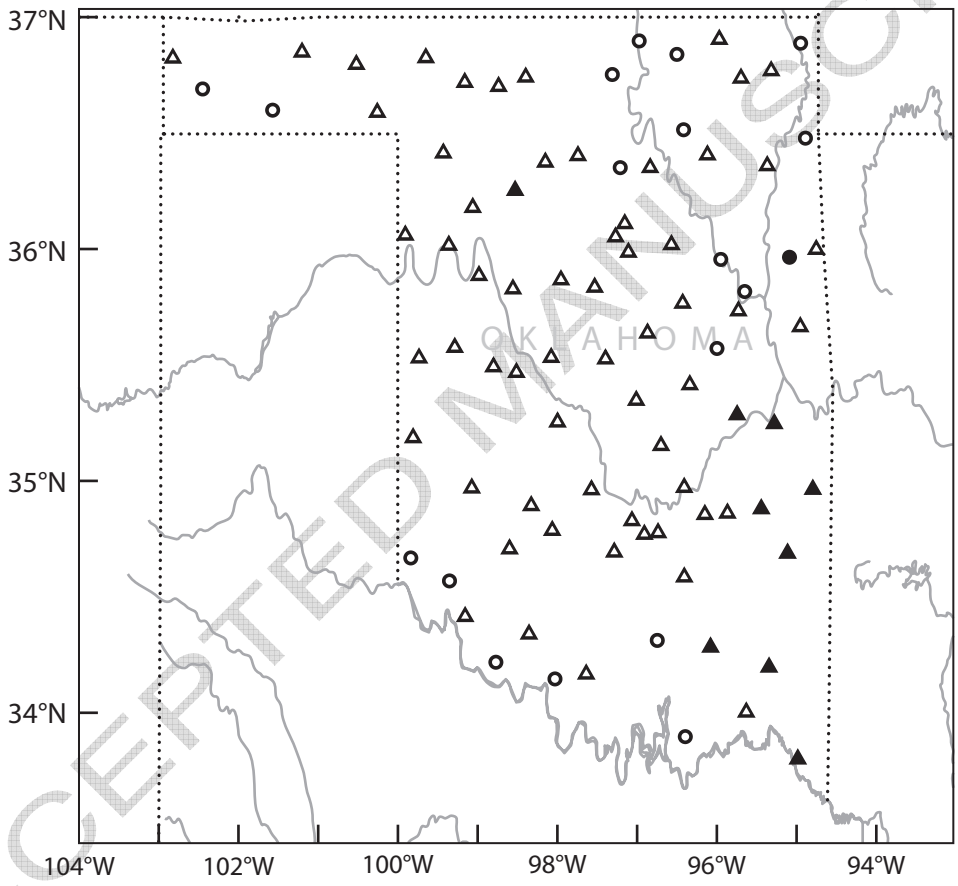

Fig. 6.

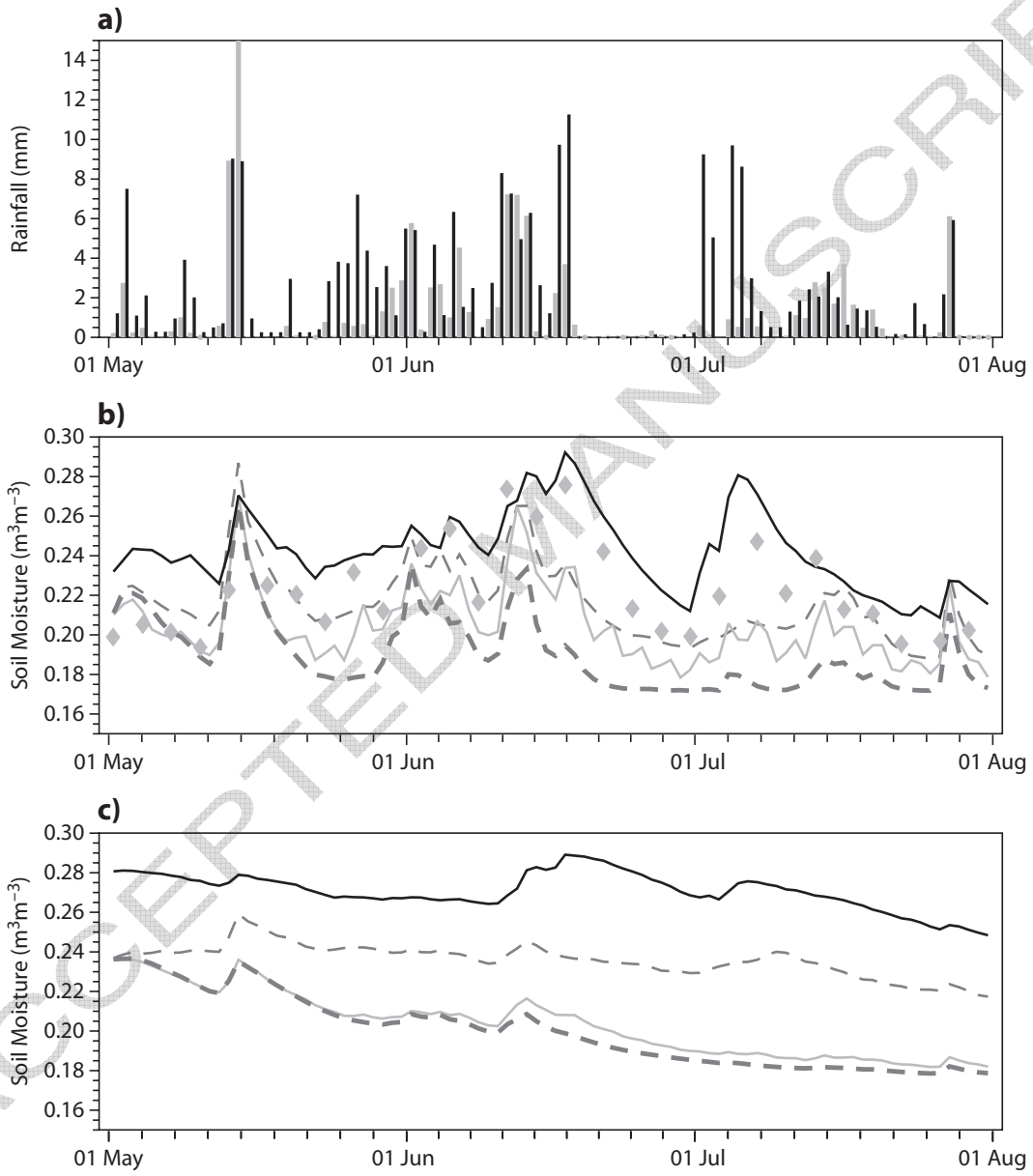

Fig. 7.

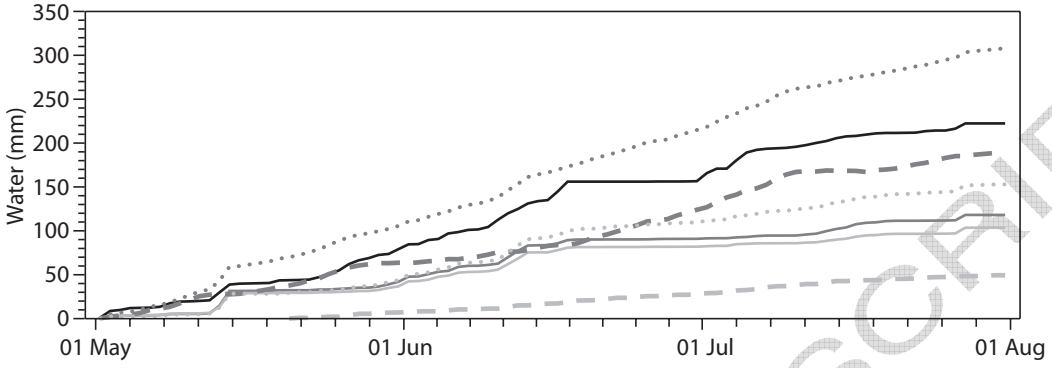

Fig. 8.

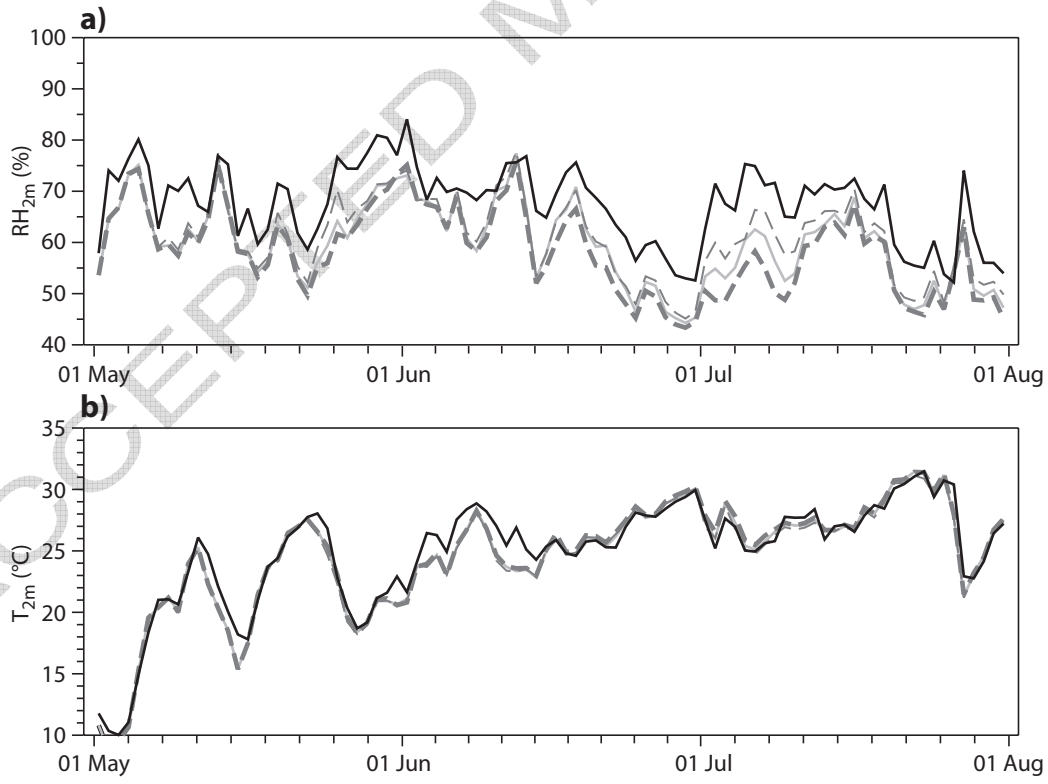

Fig. 9.

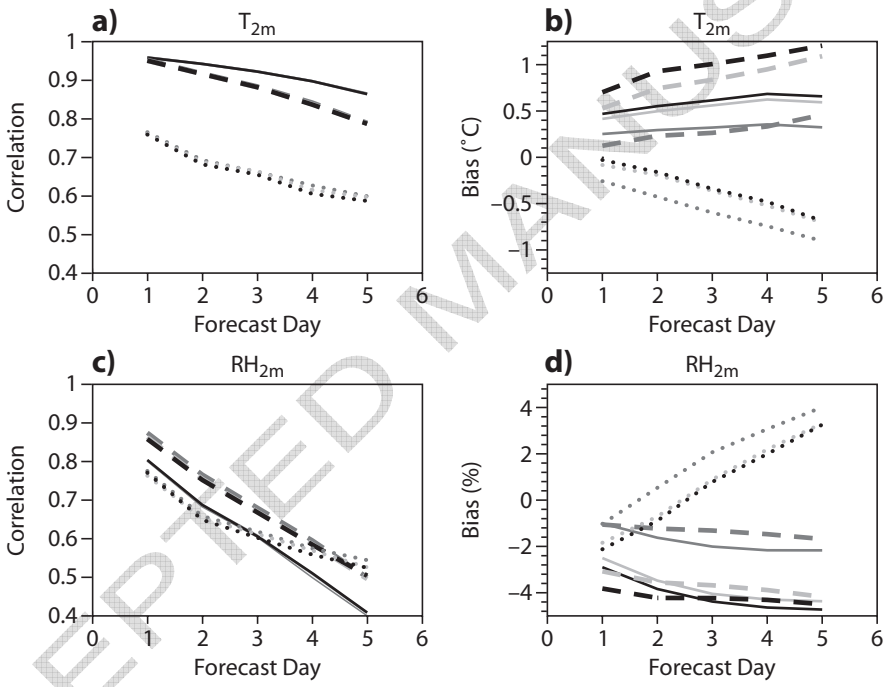

Fig. 10.